Research Article | DOI:10.5281/zenodo.8002201
www.jnanosam.com

NANOSAM
Journal of NanoScience in Advanced Materials

Magnetocaloric Effect Simulation in $La_{0.8}Na_{0.2}MnO_{3-\Delta}$ Nanopowders

Nawel Khedmi[1], Nadia Zaidi[2] and Mohamed Hsini[3#]

The critical behavior of $La_{0.8}Na_{0.2}MnO_{3-\Delta}$ nanopowders at the paramagnetic to ferromagnetic phase transition is studied. The optimized critical exponents, through an iterative program based on Kouvel–Fisher method, were found to be as: $\gamma = 1.05$; $\beta = 0.45$. These obtained critical exponents does not match with the conventional universality classes. In addition, these γ and β values are close the ones predicted by the mean-filed theory ($\gamma = 1$ and $\beta = 0.5$). It has been approved that the estimated critical temperature and the critical exponents are unambiguous and intrinsic to the $La_{0.8}Na_{0.2}MnO_{3-\Delta}$ nanopowders. Based on the combination of the Landau model and the Arrott–Noakes equation, the isothermal magnetization curves and the magnetocaloric effect have been successfully simulated.

1. Introduction

The critical behavior and the order of a phase transition analyzes are crucial to classify the dynamic behavior of magnetic materials with a lot of applications such as magnetic cooling [1], spintronics devices [2], magnetic sensors [3], magnetic storage devices [4, 5], etc. Especially, the magnetocaloric effect (MCE), needful for the magnetic refrigeration (MR) technology, manifests through a reversible temperature change in a material when it is exposed to change of magnetic field [6]. For the MR cycle, there are magnetic Stirling cycle, Brayton cycle, the Active Magnetic Regenerator Refrigeration (AMRR) cycle, Ericsson cycle, and Carnot cycle [7]. The AMRR could reach around 30-60% of Carnot efficiency with more energy-efficient and profitably. In addition, it would provide compactness, noiseless environment, and soothing environmental impact due to the solid state magnetic instead of the fluid refrigerant. The magnetic transition order has a fundamental part in practical applications of these magnetic systems. Two general properties are accompanied in this transition: the phase transition order and the universal class. Near the paramagnetic (PM) ferromagnetic (FM) phase transition, several measurable quantities could be characterized with critical temperature and exponents [8, 9]. According to the obtained exponents values, the magnetic alloys could be classified and arranged [10, 11]. Moreover, the usefulness of theoretical methods describing the MCE is substantial not only to fit the behavior of the available experimental data, but also to predict new associated properties under external or internal factors. For this goal, various recent works focus on theoretical study of the MCE [12-14]. These theoretical methodologies such as the Mean-Field Theory (MFT) [15, 16], Effective-Field Theory (EFT) [17, 18] and Monte Carlo simulation (MC) [19] set a deep description of the thermomagnetic properties of the magnetic systems.

Nowadays, the requirements shift from classical ceramic samples to nano-sized materials which can be used in biomedical application or in MCE [20]. Obviously, the particles behave as a single-domain state when the sizes of magnetic particles are reduced. This change gives rise to modify physical properties of the particles as compared to those of bulk material. Moreover, the nanoparticles physical properties are commanded by the surface disorder and the finite-size effects. It was reported that reducing size in manganites may affect their magnetic properties e.g., changing the PM to the FM transition from first to second order [21], reducing the Curie Temperature (T_C) [22, 23], favorizing the formation of an FM state at low temperature with

[1]*Al-Baha University, Faculty of Science and Arts, Physics Department, Al-Makwat, Saudi Arabia,* [2]*Jouf University, College of Sciences, Department of Physics, Aljouf, Saudi Arabia,* [3]*University of Monastir, Faculty of Science of Monastir, Laboratory of Physical Chemistry of Materials, Department of Physics, Monastir, Tunisia.*
#Corresponding author: mohamed.hsini.14@gmail.com (Mohamed Hsini)

Keywords: Critical behavior; Landau model; Magnetizations; Modified Arrott plot; Spontaneous magnetization.

Received: 09 April 2023 | Accepted: 03 June 2023 | Published online: 25 June 2023

suppressing the antiferromagnetic state [24], etc. It is generally common that compounds comprising lanthanides are feasible magnetocaloric materials [25]. Recently, Liedienov et al. [26] have reported the superparamagnetic contribution and the spin-dependent magnetism to the MCE of the $La_{0.8}Na_{0.2}MnO_3$-nanopowders (LNMO). The XRD patterns of the LNMO refined using the Rietveld method showed that the LNMO is well described in the framework of the rhombohedral space group $R\bar{3}C$. The dependence of magnetization on temperature, $M(T)$, indicated that LNMO exhibited a FM-PM at $T_C = 327\ K$. The critical behavior of LNMO was reported in [26] using relative slopes (RS) method known as $RS = S(T)/S(T_C)$, where S is the slope of the model curve under higher magnetic region. The closest model, supposing the accurate one to describe the behavior of LNMO, is reported to be the mean field model (MFM) with β = 0.5 and γ = 1, but a deviation was found between the values of the critical exponent β from the MFM value (0.5) and the obtained one (0.334) using the Kouvel–Fisher method [27]. In fact, this discrepancy returns to the limitation of the RS method to select the adequate model for a random magnetic system since it presents only four classical models: the MFM, the Tricritical Mean Field Model, the 3D-Heisenberg and the 3D-Ising Models. From the theoretical considerations, multiple models have been used for understanding different properties of materials. Some models open the access to simulate the isotherms $M(H,T)$ and the magnetic entropy change $-\Delta S_M(H,T)$ curves. The numerical resolution for the equation of the states lead to generate data. The benefit of this process could be useful to replace experimental measurements that are almost expensive and time-consuming. In this work, we studied the critical behavior of LNMO. Using a robust iterative technique [28], the critical exponents β and γ are set and sorted out again from the inverse of the magnetic susceptibility as a function of temperature $\chi_0^{-1}(T)$ and the from spontaneous magnetization as a function of temperature $M_S(T)$. Subsequently, an efficient scaling based on the combination of the Gibbs free energy with the Landau model was integrated. Based on this vigorous Landau model, isothermal magnetization $M(H,T)$ and magnetic entropy change $-\Delta S_M$ curves were successfully simulated in a wide validity temperature range. Consequently, the presented results candidate that the combination between the critical behavior and the Landau theory could be a promising theoretical method to simulate the MCE.

2. Results and Discussion

2.1. Arrott–Noakes Equation

Near a second order PM-FM phase transition, the Arrott–Noakes equation (ANE) of state, for a magnetic material with the constants a and b, is given as [29]:

$$\left(\frac{H}{M}\right)^{\frac{1}{\gamma}} = a(T - T_C) + bM^{\frac{1}{\beta}} \quad (1)$$

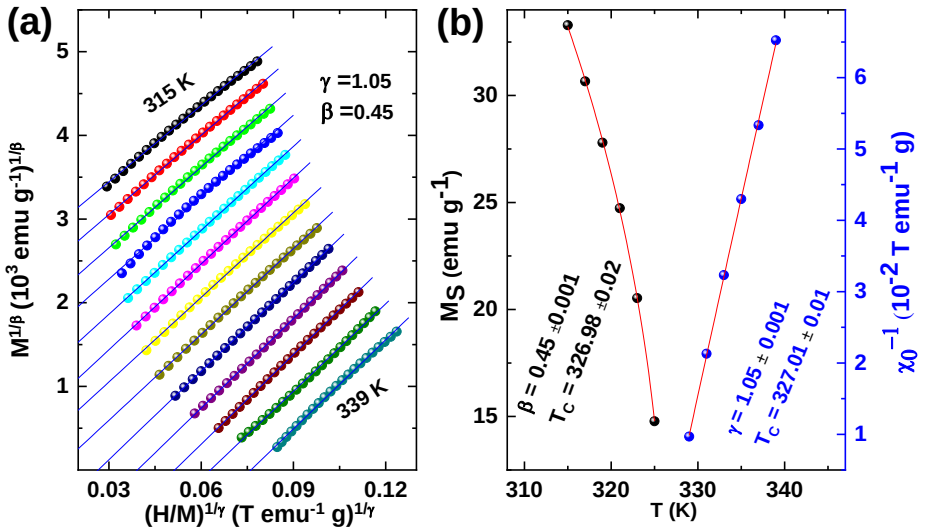

Figure 1. (a) Modified Arrot plots (MAPs), $M^{\frac{1}{\beta}}$ vs. $\left(\frac{H}{M}\right)^{\frac{1}{\gamma}}$. (b) Fitting $M_S(T)$ and $\chi_0^{-1}(T)$, with Eq. (2) and Eq. (3).

NANOSAM
Journal of NanoScience in Advanced Materials

Table 1. Critical exponents β and γ for the sample studied in this work, and values arising from known theoretical models.

Material or Model	β	γ
$La_{0.8}Na_{0.2}MnO_{3-\Delta}$ nanopowders	0.45	1.05
Mean Field Model	0.5	1
3D Heisenberg Model	0.365	1.336
3D Ising Model	0.325	1.24

Knowing that the reduced temperature is $\varepsilon = \frac{T-T_C}{T}$, the scaling relations of Eq. (1) provide M_S and χ_0^{-1} [30]:

$$M_S = M_0(-\varepsilon)^{\beta}\ ; T < T_C, \quad (2)$$

$$\chi_0^{-1} = h_0\varepsilon^{\gamma}\ ; T > T_C, \quad (3)$$

Where M_0 and h_0 are critical amplitudes. In fact, the validity of the ANE is available only in a very narrow region: $|\varepsilon| < 0.1$ [31]. The experimental isothermal data M(H, T), useful in this work, were taken from ref. [26].

The suitable β and γ values are optimized if they lead to obtain parallel straight lines for the modified Arrot plots (MAPs), $M^{\frac{1}{\beta}}$ vs. $\left(\frac{H}{M}\right)^{\frac{1}{\gamma}}$. Also, the critical isotherm (at $T = T_C$) must pass through the origin. The choice of γ and β values is not realistic because injecting two free random parameters in Eq. (1) leads to systematic errors in exponent values. To get a physical fit, an iteration program based on Kouvel–Fisher method [28] has been implemented to select the proper γ and β values. Taking γ and β arbitrarily, the implemented program will continuously modify their values until the two requirements above are achieved. The convergence in adjusting is reached with $\gamma = 1.05$ and $\beta = 0.45$ for LNMO. Using these last values, a nice plot showing parallel straight lines in Fig. 1(a) was generated. It is significant to mention that during critical scaling in Fig. (1a) only the higher fields region ($H > 1$ T) are considered because of the rearrangement of magnetic domains at the lower fields and the demagnetization factor that affect the MAPs with deviation from linearity [32].Linear fits of the MAP give $M_S^{1/\beta}$ and $(\chi_0^{-1})^{1/\gamma}$. The obtained $M_S(T)$ and $\chi_0^{-1}(T)$ for LNMO are represented in Fig. 1(b). Fitting $M_S(T)$ using Eq. (2) gives: $\beta = 0.45$ and $T_C = 326.98$ K. However, fitting $\chi_0^{-1}(T)$ using Eq. (3) gives: $\gamma = 1.05$ and $T_C = 327.01$ K. The obtained critical exponents for the $La_{0.8}Na_{0.2}MnO_{3-\Delta}$ nanopowders are compared with the ones arising from known theoretical models (see Table 1).

As shown in Table 1, the obtained β and γ of $La_{0.8}Na_{0.2}MnO_{3-\Delta}$ nanopowders does not match with universal classes. But these γ and β values are close to the ones predicted by the mean-filed theory ($\gamma = 1$ and $\beta = 0.5$). This critical behavior analysis confirms that the obtained critical values are unambiguous and intrinsic to the $La_{0.8}Na_{0.2}MnO_{3-\Delta}$ nanopowders.

2.2 Critical exponents and Landau models

The Gibbs free energy for a random FM system with a second order transition can be expressed within the Landau model as [32]:

$$G(T, M) = G_0 + \left[\frac{1}{\frac{1}{\gamma}+1}A(T)M^{\frac{1}{\gamma}+1} + \frac{1}{\frac{1}{\beta}+\frac{1}{\gamma}+1}B(T)M^{\frac{1}{\beta}+\frac{1}{\gamma}+1} - MH^{\frac{1}{\gamma}}\right]H^{1-\frac{1}{\gamma}} \quad (4)$$

where G_0 is the reference energy, A(T) and B(T) are parameters depending on temperature and containing electron condensation energy and magnetoelastic coupling [33]. The minimization of the Gibbs free energy, $\left(\frac{dG}{dM}\right)_T = 0$, leads to obtain the following equation of the state:

$$\left(\frac{H}{M}\right)^{\frac{1}{\gamma}} = A(T) + B(T)M^{\frac{1}{\beta}} \quad (5)$$

However, the magnetic entropy $\left(S_M = -\frac{dG}{dT}\right)$ with eliminating M_S values [34] can be expressed as:

$$-\Delta S_M = \left[\frac{1}{\frac{1}{\gamma}+1}\frac{dA(T)}{dT}\left(M^{\frac{1}{\gamma}+1} - M_S^{\frac{1}{\gamma}+1}\right) + \frac{1}{\frac{1}{\beta}+\frac{1}{\gamma}+1}\frac{dB(T)}{dT}\left(M^{\frac{1}{\beta}+\frac{1}{\gamma}+1} - M_S^{\frac{1}{\beta}+\frac{1}{\gamma}+1}\right) - (M - M_S)H^{\frac{1}{\gamma}}\right]H^{1-\frac{1}{\gamma}} \quad (6)$$

With the reliable γ and β values estimated above, isotherms $\left(\frac{H}{M}\right)^{\frac{1}{\gamma}}$ vs. $M^{\frac{1}{\beta}}$ at the hole temperature range and under high magnetic fields for the LNMO are plotted in Fig. 2.

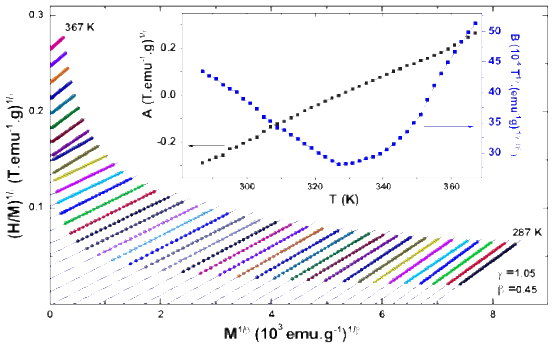

Figure 2. The linear fits of $\left(\frac{H}{M}\right)^{\frac{1}{\gamma}}$ vs. $M^{\frac{1}{\beta}}$. The inset presents the corresponding A(T) and B(T) curves.

NANOSAM
Journal of NanoScience in Advanced Materials

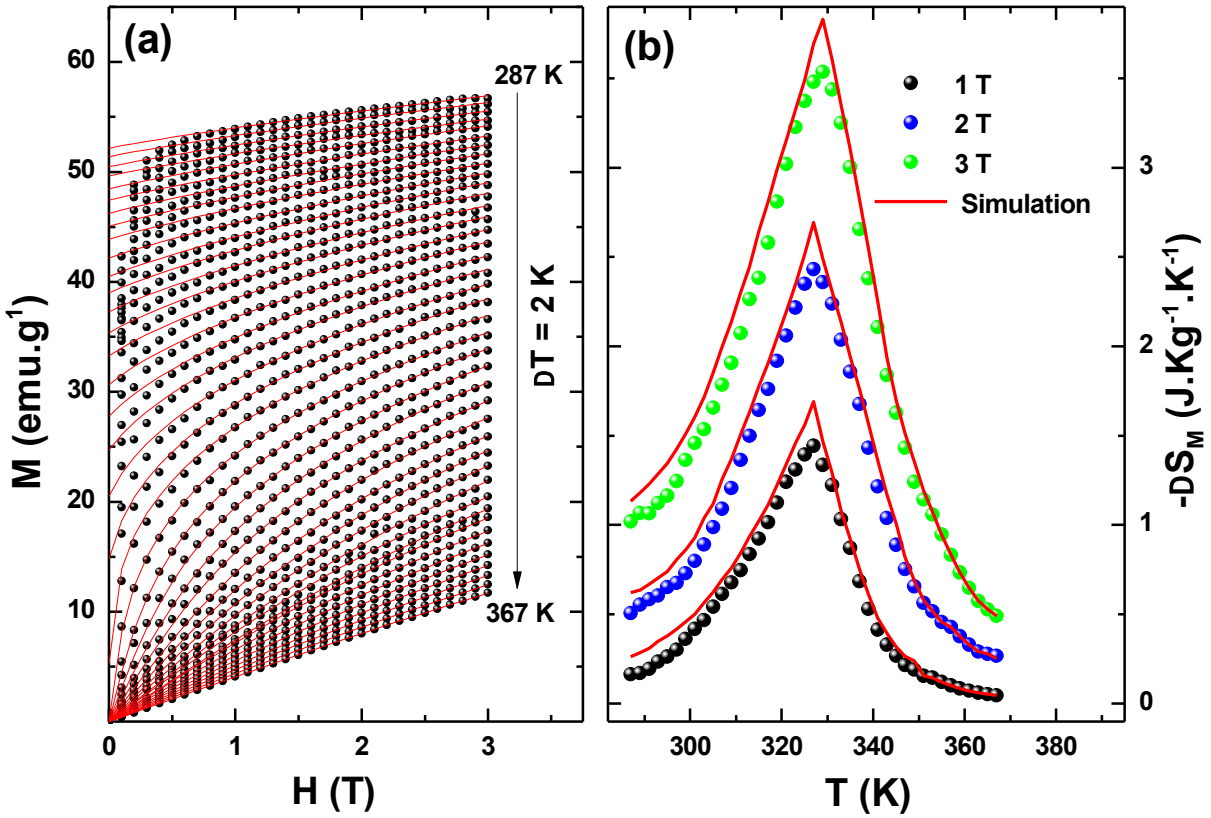

Figure 3. Simulation (with red lines) of (a) isotherms M(H, T) and (b) $-\Delta S_M(T)$ curves under various H values using the Landau model. The corresponding experimental results [26] are shown with symbols.

According to Eq. (7), linear fittings of $\left(\frac{H}{M}\right)^{\frac{1}{\gamma}}$ vs. $M^{\frac{1}{\beta}}$ give A(T) and B(T) curves which are shown in the inset of Fig. 2. At $T = T_C$, $A(T_C) = 0$; $\left.\frac{\partial A}{\partial T}\right|_{T_C} \neq 0$; $B(T_C) \neq 0$ and $\left.\frac{\partial B}{\partial T}\right|_{T_C} = 0$. These criteria are similar with a second order magnetic transition as reported Amaral et al. [35].

Resolving Eq. (5) with the known A(T) and B(T) may generate isothermal M(H, T) curves which are represented with red lines in Fig. 3(a). Simulated M(H, T) curves correlate with the experimental data (symbols).

The generated M(H, T) and the calculated M_S with the γ and β values are inserted in Eq. (6) to generate $-\Delta S_M(T)$ curves. These $-\Delta S_M(T)$ curves (red lines) are displayed in Fig. 3 and compared with the corresponding experimental ones (symbols) for the LNMO.

A well correlation between simulated and experimental $-\Delta S_M(T)$ curves is set in a large temperature range which confirms the promising of such theoretical models to simulate the MCE in LNMO.

3. Conclusion

To conclude, the present study reports critical behavior across the paramagnetic ferromagnetic transition for the $La_{0.8}Na_{0.2}MnO_{3-\Delta}$ nanopowders. The values of the critical exponents γ and β were optimized as to be1.05 and 0.45, respectively. They were exploited to analyze the Gibbs free energy within the Landau theory. As a result, isothermal magnetization and the magnetic entropy change curves were successfully simulated from this analysis. Based on the renormalization-group study, this critical behavior analysis may help to understand the exchange interactions, for the $La_{0.8}Na_{0.2}MnO_{3-\Delta}$ nanopowders.

Method

Isothermal magnetization data were analyzed using MATLAB software. Resolving the equations of the state is achieved using methods based on the nonlinear least-squares algorithms. If the system may not have a zero, the algorithm still returns a point where the residual is small.

Acknowledgements

Not applicable.

Authors' contributions:

The manuscript was written with the contributions of all authors. NK contributed to preparing experimental data and editing of the manuscript. NZ contributed to reviewing and editing of the manuscript. MH contributed to calculations.

Data Availability Statement

There are no conflicts to declare. The datasets generated or analyzed during the current study are available from the corresponding author on reasonable request.

References

[1] Al-Yahmadi, I.Z., Gismelseed, A.M., Al Ma'Mari, F., Al-Rawas, A.D., Al-Harthi, S.H., Yousif, A.Y., Widatallah, H.M., Elzain, M.E., Myint, M.T.Z., Structural, magnetic and magnetocaloric effect studies of Nd0.6Sr0.4AxMn1-xO3 (A=Co, Ni, Zn) perovskite manganites, Journal of Alloys and Compounds **875** 159977 (2021).

[2] Xie, K., Wang, J., Xu, S., Hao, W., Zhao, L., Huang, L., Wei, Z.J.M., Design, Application of Two-Dimensional MXene materials in sensors, **228** 111867 (2023).

[3] Zhang, Y., Zhu, J., Li, S., Zhang, Z., Wang, J., Ren, Z.J.S.C.M., Magnetic properties and promising magnetocaloric performances in the antiferromagnetic GdFe2Si2 compound, **65** (5) 1345-1352 (2022).

[4] Guo, D., Moreno-Ramírez, L.M., Law, J.-Y., Zhang, Y., Franco, V.J.S.C.M., Excellent cryogenic magnetocaloric properties in heavy rare-earth based HRENiGa2 (HRE= Dy, Ho, or Er) compounds, **66** (1) 249-256 (2023).

[5] Xia, W., Pei, Z., Leng, K., Zhu, X.J.N.R.L., Research progress in rare earth-doped perovskite manganite oxide nanostructures, **15** (1) 1-55 (2020).

[6] Lyubina, J.J.J.o.P.D.A.P., Magnetocaloric materials for energy efficient cooling, **50** (5) 053002 (2017).

[7] Silva, D.J., Ventura, J., Araújo, J.P.J.I.J.o.E.R., Caloric devices: A review on numerical modeling and optimization strategies, **45** (13) 18498-18539 (2021).

[8] Li, Y., Feng, S., Lv, Q., Kan, X., Liu, X.J.J.o.A., Compounds, An investigation of reentrant spin-glass behavior, magnetocaloric effect and critical behavior of MnCr2O4, **877** 160224 (2021).

[9] Ahmed, A., Mazumdar, D., Das, K., Das, I.J.J.o.M., Materials, M., A comparative study of the magnetic and magnetocaloric effect of polycrystalline Gd0. 9Y0. 1MnO3 and Gd0. 7Y0. 3MnO3 compounds: Influence of Y-ions on the magnetic state of GdMnO3, **551** 169133 (2022).

[10] Ma, K.J.A.B.I., Modern Theory of Critical Phenomena, Ed, (1976).

[11] Huang, K., Statistical mechanics, John Wiley & Sons (2008).

[12] Hsini, M., Hcini, S., Zemni, S.J.J.o.M., Materials, M., Magnetocaloric effect studying by means of theoretical models in Pr0. 5Sr0. 5MnO3 manganite, **466** 368-375 (2018).

[13] Masrour, R., Jabar, A., Khlif, H., Jemaa, F.B., Ellouze, M., Hlil, E.J.S.s.c., Experiment, mean field theory and Monte Carlo simulations of the magnetocaloric effect in La0. 67Ba0. 22Sr0. 11MnO3 compound, **268** 64-69 (2017).

[14] Igoshev, P.A., Nekrasov, I.A., Pavlov, N.S., Chinyaev, T.H., Yakupov, E.O., Investigation of magnetocaloric effect: Stoner approximation vs DMFT, Journal of Physics: Conference Series, IOP Publishing, pp. 012083 (2019).

[15] Amaral, J., Amaral, V.J.J.o.m., materials, m., On estimating the magnetocaloric effect from magnetization measurements, **322** (9-12) 1552-1557 (2010).

[16] Amaral, J., Silva, N., Amaral, V.J.A.P.L., A mean-field scaling method for first-and second-order phase transition ferromagnets and its application in magnetocaloric studies, **91** (17) 172503 (2007).

[17] Vatansever, E., Akinci, Ü., Yüksel, Y.J.P.A.S.M., Applications, i., Non equilibrium magnetocaloric properties of Ising model defined on regular lattices with arbitrary coordination number, **479** 563-571 (2017).

[18] Akıncı, Ü., Yüksel, Y., Vatansever, E.J.P.L.A., Magnetocaloric properties of the spin-S (S≥ 1) Ising model on a honeycomb lattice, **382** (45) 3238-3243 (2018).

[19] Buchelnikov, V., Sokolovskiy, V., Taskaev, S., Khovaylo, V., Aliev, A., Khanov, L., Batdalov, A., Entel, P., Miki, H., Takagi, T.J.J.o.P.D.A.P., Monte Carlo simulations of the magnetocaloric effect in magnetic Ni–Mn–X (X= Ga, In) Heusler alloys, **44** (6) 064012 (2011).

[20] Liedienov, N., Kalita, V., Pashchenko, A., Dzhezherya, Y.I., Fesych, I., Li, Q., Levchenko, G.J.J.o.A., Compounds, Critical phenomena of magnetization, magnetocaloric effect, and superparamagnetism in nanoparticles of non-stoichiometric manganite, **836** 155440 (2020).

[21] Xi, S., Lu, W., Sun, Y.J.J.o.A.P., Magnetic properties and magnetocaloric effect of La0. 8Ca0. 2MnO3 nanoparticles tuned by particle size, **111** (6) 063922 (2012).

[22] Biswas, A., Das, I.J.J.o.A.P., Magnetic and transport properties of nanocrystalline Nd 0.5 Sr 0.5 MnO 3, **102** (6) 064303 (2007).

[23] Mathew, S., Kaul, S.J.a.p.l., Tuning magnetocaloric effect with nanocrystallite size, **98** (17) 172505 (2011).

[24] Rao, S., Bhat, S.J.J.o.P.C.M., Probing the existing magnetic phases in Pr0. 5Ca0. 5MnO3 (PCMO) nanowires and nanoparticles: magnetization and magneto-transport investigations, **22** (11) 116004 (2010).

[25] Pena, C., Soffner, M., Mansanares, A., Sampaio, J., Gandra, F., da Silva, E., Vargas, H.J.P.B.C.M., Structural and magnetic analysis of La0. 67Ca0. 33MnO3 nanoparticles thermally treated: Acoustic detection of the magnetocaloric effect, **523** 39-44 (2017).

[26] Liedienov, N.A., Wei, Z., Kalita, V.M., Pashchenko, A.V., Li, Q., Fesych, I.V., Turchenko, V.A., Hou, C., Wei, X., Liu, B.J.A.M.T., Spin-dependent magnetism and superparamagnetic contribution to

the magnetocaloric effect of non-stoichiometric manganite nanoparticles, **26** 101340 (2022).

[27] Kouvel, J.S., Fisher, M.E.J.P.R., Detailed magnetic behavior of nickel near its Curie point, **136** (6A) A1626 (1964).

[28] Pramanik, A., Banerjee, A.J.P.R.B., Critical behavior at paramagnetic to ferromagnetic phase transition in Pr 0.5 Sr 0.5 MnO 3: A bulk magnetization study, **79** (21) 214426 (2009).

[29] Arrott, A., Noakes, J.E.J.P.R.L., Approximate equation of state for nickel near its critical temperature, **19** (14) 786 (1967).

[30] Fisher, M.E.J.R.o.p.i.p., The theory of equilibrium critical phenomena, **30** (2) 615 (1967).

[31] Zhang, L., Fan, J., Zhang, Y.J.M.P.L.B., Magnetic entropy calculation for a second-order ferromagnetic phase transition, **28** (08) 1450059 (2014).

[32] Cabassi, R., Bolzoni, F., Gauzzi, A., Licci, F.J.P.R.B., Critical exponents and amplitudes of the ferromagnetic transition in La 0.1 Ba 0.9 V S 3, **74** (18) 184425 (2006).

[33] Lévy, L.-P., Magnetism and superconductivity, Springer Science & Business Media (2000).

[34] Dong, Q.-y., Zhang, H.-w., Shen, J.-l., Sun, J.-r., Shen, B.-g.J.J.o.m., materials, m., Field dependence of the magnetic entropy change in typical materials with a second-order phase transition, **319** (1-2) 56-59 (2007).

[35] Amaral, V., Amaral, J.J.J.o.m., materials, m., Magnetoelastic coupling influence on the magnetocaloric effect in ferromagnetic materials, **272** 2104-2105 (2004).